Polarization-Corrected Electrostatic Potential for Probing Cation Binding Patterns of Molecules. 1. Saturated Hydrocarbons

Shridhar R. Gadre* and Subhash S. Pingale

Contribution from the Department of Chemistry, University of Pune, Pune-411 007, India

Received May 12, 1997. Revised Manuscript Received February 2, 1998

Abstract: The molecular electrostatic potential (MESP) and the corresponding polarization corrected one (PMESP) of some saturated hydrocarbons, viz., methane, ethane, cyclopropane, cyclobutane, *n*-butane, and cyclohexane, have been examined at the ab initio SCF level. The topography of PMESP has been employed for predicting coordination of Li^+ with these hydrocarbons. Coordination site of Li^+ usually turns out to be in the direction guided by the corresponding PMESP critical points (CPs) of these hydrocarbons. An ab initio level minimum energy search along this direction is used to generate possible starting configurations of hydrocarbon···Li^+ complexes. Hartree−Fock and second-order Møller−Plesset (MP2) calculations with 6-31G** basis set are performed with these starting geometries for investigating the structures and energetics of the complexes. A remarkable correlation has been found between the PMESP values at CPs and the corresponding Li^+ binding energies. General trends in geometries and interaction energies of the hydrocarbon···Li^+ complex structures obtained at the HF level are almost unaffected by electron correlation as well as extension of the basis set beyond 6-31G**. The Kitaura−Morokuma energy decomposition analysis brings out the importance of the polarization term, while the electrostatic term is seen to dominate selectively for cyclopropane. Complete exploitation of three-dimensional PMESP distribution thus offers a systematic way for studying cation···molecule interactions.

Introduction

Interaction of metal cation with organic molecules has been an active area of research for the past several years.[1] In particular, the study of hydrocarbon−metal cation interactions has received considerable attention in the recent years.[2] These studies are very vital for exploring the activation of hydrocarbons by metal cations.[2a] The ultimate goal of these works is to obtain valuable hints on the mechanism of stoichiometric or catalytic processes, solely from the intrinsic properties of the bare metal cation and the respective neutral molecule. The activation of C−H or C−C bonds in alkanes and understanding the detailed mechanism for reaction propagation and termination still remains a formidable challenge in homogeneous or heterogeneous catalysis.[2a,b] In this connection, Hankinson et al.[1a] conjectured that the metal ion must be close to a bond for chemistry involving that bond to occur. In summary, the patterns of binding in cation-hydrocarbon systems are of great theoretical and practical interest. Hankinson et al.,[1a] Radecki et al.,[3a] and Tsarbopoulos et al.[3b] have suggested that the geometry of the initial ion/molecule complex that is formed has a strong influence on where the metal will insert. It is suggested that the final products and their distributions would be simple to predict[3c] from the knowledge of initial interaction intermediates. Hankinson et al.[1a] concluded, by modeling the ion−molecule complexes, that the first step in the reaction, viz., complexation, may be a key factor in determining which bonds are likely to be preferentially attacked and hence in deciding the final product distributions.

It has also been argued that complexes of organic molecules with metal cation are electrostatic in origin, and this complexation may be crucial in controlling the final product distribution.[1a,2f,g,h,4−7] Interactions of metal cation with biological molecules, especially cation-π interaction with bio-organic molecules,[6b,8] is also a vigorously pursued area of contemporary research.

Alkali-metal cation systems provide a good illustration of ion−molecule complexes in gas phase which are essentially electrostatic, dominated by ion−dipole interactions with further

(1) Hankinson, D. J.; Allison, J. *J. Phys. Chem.* **1987**, *91*, 5307. (b) Allison, J. *Prog. Inorg. Chem.* **1986**, *34*, 627.

(2) (a) Eller, K.; Schwarz, H. *Chem. Rev.* **1991**, *91*, 1121. (b) Mourgues, P.; Ferhati, A.; McMahon, T. B.; Ohanessian, G. *Organometallics* **1997**, *16*, 210. (c) Schroeter, K.; Schalley, C. A.; Wesendrup, R.; Schroder, D.; Schwarz, H. *Organometallics* **1997**, *16*, 986. (d) Smith, G. D.; Jaffe, R. L.; Partridge, H. *J. Phys. Chem. A* **1997**, *101*, 1705. (e) Hendrickx, M.; Ceulemans, M.; Vanquickenborne, L. *Chem. Phys. Lett.* **1996**, *257*, 8. (f) Carroll, J. J.; Haug, K. L.; Weisshaar, J. C.; Blomberg, M. R. A.; Siegbahn, P. E. M.; Svensson M. *J. Phys. Chem.* **1995**, *99*, 13955. (g) Hill, Y. D.; Freiser, B. S.; Bauschlicher, C. W. Jr. *J. Am. Chem. Soc.* **1991**, *113*, 1507. (h) Rosi, M.; Bauschlicher, C. W., Jr. *Chem. Phys. Lett.* **1990**, *166*, 189. (i) Crellin, K. C.; Geribaldi, S.; Widmer, M.; Beauchamp, J. L *Organometallics* **1995**, *14*, 4366. (j) Cornehl, H. H.; Heinemann, C.; Schröder, D.; Schwarz, H. *Organometallics*, **1995**, *14*, 992. (k) Ranasinghe, Y. A.; MacMahon, T. J.; Freiser, B. S. *J. Am. Chem. Soc.* **1992**, *114*, 9112. (l) Hendrickx, M.; Ceulemans, M.; Gong, K.; Vanquickenborne, L. *J. Phys. Chem. A* **1997**, *101*, 2465.

(3) (a) Radecki, B. D.; Allison, J. *Organometallics* **1986**, *5*, 411. (b) Tsarbopoulos, A.; Allison, J. *J. Am. Chem. Soc.* **1985**, *107*, 5085. (c) Tsarbopoulos, A.; Allison, J. *Organometallics* **1984**, *3*, 86.

(4) Alcamí, M.; Mó, O.; Yáñez, M. *J. Am. Chem. Soc.* **1993**, *115*, 11074.

(5) (a) Dougherty, D. A. *Science* **1996**, *271*, 163. (b) Mecozzi, S.; West, A. P. Jr.; Dougherty, D. A. *J. Am. Chem. Soc.* **1996**, *118*, 2307.

(6) (a) van Koppen, P. A. M.; Brodbelt-Lusting, J.; Bowers, M. T.; Dearden, D. V.; Beauchamp, J. L.; Fisher, E. R.; Armentrout, P. B. *J. Am. Chem. Soc.* **1991**, *113*, 2359. (b) Caldwell, J. W.; Kollman, P. A. *J. Am. Chem. Soc.* **1995**, *117*, 4177.

(7) (a) Cimiraglia, R.; Tomasi, J.; Cammi, R.; Hofmann, H.-J. *Chem. Phys.* **1989**, *136*, 399. (b) Ray, D.; Feller, D.; More, M. B.; Glendening, E. D.; Armentrout, P. B. *J. Phys. Chem.* **1996**, *100*, 16116. (c) More, M. B.; Glendening, E. D.; Ray, D.; Feller, D.; Armentrout, P. B. *J. Phys. Chem.* **1996**, *100*, 1605. (d) Tian, F.; Lee, K.-C.; Hu, W.; Cross, T. A. *Biochemistry* **1996**, *35*, 11959.

S0002-7863(97)01544-8 CCC: $15.00
Published on Web 06/29/1998

enhancement by the polarization term.[4,9] Smith et al.[2d] have found that a simple force field with two-body interaction potential functions representing induction or polarization effects could reproduce the respective ab initio complex energies reasonably well for single ligand complexes.

It has been remarked that a metal cation prefers to interact along a direction which corresponds to the negative end of the molecular dipole moment vector, and this type of interaction is predominantly governed by ion−dipole and polarization interactions because of the greater ionic character of the bond to the metal cation.[7a] The works by Hill et al.[2g], Caldwell at al.,[6b] Ray at al.,[7b] and Hankinson et al.[1a] have demonstrated that for metal cation···hydrocarbon complexes electrostatic interaction as well as polarizability effects are important to more or less extent. Dykstra's[10] work stresses the predominance of intermolecular interactions in complexes by the electrostatics and higher multipole moments.

Several years ago, Politzer et al.[11] have shown that in hydrocarbons, CH_3 and CH_2 groups can give rise to negative electrostatic potential. In the several earlier studies[12] since 1970, the molecular electrostatic potential (MESP) produced by the molecular distribution has been calculated and employed successfully for predicting the molecular sites susceptible to an electrophilic attack. Till recent years,[5b,8c,13,14] this has formed a useful approach for understanding cation−molecule interactions. Goldfuss et al.[13] have shown that MESP provides a basis for the unusually high Li^+ edge coordination energy to cyclopropane. With theoretical calculations, they have thus obtained two local minimum energy structures on the potential energy surface. But this electrostatic argument cannot explain why in the cyclopropane···Li^+ complex, Li^+ can bind from the top side of the cyclopropane ring, since the negative valued MESP zone is conspicuous by its absence[14c] on its C_3 axis. Also it has been found[2g] that the cations are bonded to ethane along a line perpendicular to the C−C bond of ethane. For this case also, the MESP fails to provide an acceptable qualitative explanation, since from the MESP topographical study it is observed that there is no significantly negative MESP zone in the region perpendicular to the C−C bond.[14c] Hill et al.[2g] have commented that the binding energy of Li^+ for saturated and unsaturated hydrocarbons generally increases with the size of the hydrocarbon due to larger relaxation and polarization effects, a conjecture which remains to be further checked.

Alcamí et al.[14f] emphasize that in those cases where the interaction of a neutral molecule with the cation involves a significant structural change in the former, the MESP fails to predict correctly the preferred site for electrophilic attack.

Polarization-corrected MESP (PMESP) has been employed for predicting the sites of electophilic[15] as well as nucleophilic attack[16] in a variety of systems. In view of this, along with the failure of MESP for some cases as reported above, a rigorous mapping of MESP followed by investigation of a polarization-corrected one seems to be important. Such an approach is felt worthwhile, since a more complete picture of the cation··· hydrocarbon interactions is expected to be thereby obtained.

The principal objectives of such an approach may thus be summarized as follows. (1) Investigate the electron localization patterns in aliphatic and alicyclic hydrocarbons. (2) Guess the potent site for incoming metal cation (Li^+) with the help of PMESP topography of saturated hydrocarbons. (3) Predict, by using ab initio docking based model, the possible complex structures and further utilize these structures as an initial guess for a fuller ab initio treatment. (4) Estimate the barrier to lithium ion transfer in systems having two or more local minima on the potential energy surface.

The next section describes the methodology employed in the present work.

Methodology

The MESP, $V(\mathbf{r})$, produced by a molecular charge distribution is defined as

$$V(\mathbf{r}) = \sum \frac{Z_A}{|\mathbf{R}_A - \mathbf{r}|} - \sum_{\mu}\sum_{\nu} D_{\mu\nu} \int d\mathbf{r}' \chi_\mu(\mathbf{r}') \frac{1}{|\mathbf{r}' - \mathbf{r}|} \chi_\nu(\mathbf{r}') \tag{1}$$

where, $D_{\mu\nu}$ are the density matrix elements in the basis of the atomic orbitals (AO) χ_μ and Z_A is the charge of the nucleus A.

If this charge distribution is perturbed by an exterior charge Q, then the polarization term, V_{PL}, in the perturbation theoretical framework applied to SCF approximation,[15,16] is given by

$$V_{PL}(\mathbf{r}) = Q^2 \sum_{i}^{occ}\sum_{a}^{vir} (\epsilon_i - \epsilon_a)^{-1} \left[\sum_{\mu}\sum_{\nu} C_{\mu i} C_{\nu a} \int d\mathbf{r}' \chi_\mu(\mathbf{r}') \frac{1}{|\mathbf{r}' - \mathbf{r}|} \chi_\nu(\mathbf{r}')\right]^2 \tag{2}$$

where ϵ_i and $C_{\mu i}$ are the MO eigenvalues and eigenvectors in the basis of the AOs $\{\chi_\mu\}$. The total PMESP is calculated as a sum

$$V_{PLC}(\mathbf{r}) = V(\mathbf{r}) + V_{PL}(\mathbf{r}) \tag{3}$$

This polarization-corrected MESP, viz., PMESP, $V_{PLC}(\mathbf{r})$, can be used to probe whether the nuclear or electronic effect including polarization is dominant at a given point. Three-dimensional information regarding PMESP is furnished by its topographical analysis. Such an analysis is based on identification and location of critical points (CPs), i.e., points where the gradient of PMESP vanishes.

(8) (a) Stöckigt, D. J. *Phys. Chem. A* **1997**, *101*, 3800. (b) Kumpf, R. A.; Dougherty, D. A. *Science* **1993**, *261*, 1708. (c) Mecozzi, S.; West, A. P. Jr.; Dougherty, D. A. *Proc. Natl. Acad. Sci. U.S.A.* **1996**, *93*, 10566. (d) Cerda, B. A.; Wesdemiotis, C. *J. Am. Chem. Soc.* **1996**, *118*, 11884. (e) Ma, J. C.; Dougherty, D. A. *Chem. Rev.* **1997**, *97*, 1303. (f) Kearney, P. C.; Mizoue, L. S.; Kumpf, R. A.; Forman, J. E.; McCurdy, A.; Dougherty, D. A. *J. Am. Chem. Soc.* **1993**, *115*, 9907.

(9) Alcamí, M.; Mó, O.; Yáñez, M. *J. Phys. Chem.* **1992**, *96*, 3022.

(10) Dykstra, C. E.; *Chem. Rev.* **1993**, *93*, 2339.

(11) Politzer, P.; Daiker, K. C.; *Chem. Phys. Lett.* **1975**, *34*, 294.

(12) (a) Bonaccorsi, R.; Scrocco, E.; Tomasi, J. *J. Chem. Phys.* **1970**, *52*, 5270. (b) Orita, Y.; Pullman, A. *Theor. Chim. Acta (Berl.)* **1977**, *46*, 251. (c) Orita, Y.; Pullman, A. *Theor. Chim. Acta (Berl.)* **1977**, *45*, 257. (d) Politzer, P.; Murray, J. S. *Structure and Reactivity*; Liebman, J. F., Greenberg, A., Eds.; VCH: 1988; Chapter 1. (e) Scrocco, E.; Tomasi, J. *Topics in Current Chemistry*; Springer, Berlin, 1973; p 42. (f) Scrocco, E.; Tomasi, J. *Adv. Quantum Chem.* **1978**, *11*, 115.

(13) Goldfuss, B.; Schleyer, P. v. R.; Hampel, F. *J. Am. Chem. Soc.* **1996**, *118*, 12183.

(14) *Molecular Electrostatic Potentials: Concepts and Applications;* Murray, J. S., Sen, K., Eds.; Elsevier: Amsterdam, 1996. In particular, see the following articles in this monograph: (a) Tomasi, J.; Mennucci, B.; Cammi, R. p 1. (b) Orozco, M.; Luque, F. J. p 181. (c) Gadre, S. R.; Bhadane, P. K.; Pundlik, S. S.; Pingale, S. S. p 219. (d) Mishra, P. C.; Kumar, A. p 257. (e) Náray-Szabó, G. p 333. (f) Alcamí, M.; Mó, O.; Yáñez, M. p 407.

(15) Dehareng, D.; Dive, G.; Ghuysen, J. M. *J. Am. Chem. Soc.* **1993**, *115*, 6877.

(16) (a) Francl, M. M. *J. Phys. Chem.* **1985**, *89*, 428. (b) Dive, G.; Dehareng, D. *Int. J. Quantum Chem.* **1993**, *46*, 127. (c) Alkorta, I.; Perez, J. J.; Villar, H. O. *J. Mol. Graphics* **1994**, *12*, 3.

In the present work, ab initio wave functions at the HF/6-31G** level obtained using the GAMESS[17] package have been employed for the evaluation[18] of the MESP and PMESP distributions of aliphatic and alicyclic hydrocarbons. The PMESP topographical analysis is carried out numerically, whereas that for MESP is done[18] by using algebraic formulas for derivatives. The PMESP values have been computed on 3-D grid points generated by step size 0.01 au for a topographical investigation. Finally, a tolerance factor of 10^{-4} au is used in the PMESP critical point search for each of individual Cartesian gradients, which are evaluated numerically.[19]

Gadre et al.[14c,20] have recently demonstrated that negative-valued CPs of MESP lie quite close to the van der Waals envelope of molecule, whereas PMESP CPs are known to be quite deep[15] in value and closer to the nuclei in the molecule. Kulkarni et al.[21] have found that expansion of the basis set beyond 6-31G** level as well as incorporating electron correlation does not generally result in significant change in the MESP topography. Similarly, Alkorta et al.[22] observed that qualitative trends in PMESP are similar for different basis sets. Hence, a*b initio* HF/6-31G** level docking of Li^+ as a key with saturated hydrocarbons (methane, ethane, cyclopropane, cyclobutane, *n*-butane, and cyclohexane) treated as a lock is carried out as guided by the corresponding PMESP CPs. Docking is carried out by only translation of Li^+, in the direction of the PMESP CPs. During this docking, the internal geometries of the hydrocarbons are held fixed, and structures of $Li^+\cdots$ hydrocarbon complexes are obtained by minimizing the ab initio docking energy (E_{dock}) by moving Li^+ **along a direction** as discussed above. The ΔE_{dock} is defined as the difference between the best docked ab initio energy of the complex and the sum of the energies of two individual species. ΔE_{SCF} and ΔE_{MP2} are defined similarly with reference to the fully optimized geometries of the complex at SCF and MP2 level, respectively. These geometries (docking geometries) are used subsequently as starting guesses for further full optimization within the ab initio framework. The full ab initio optimization of $Li^+\cdots$ hydrocarbon complexes was carried out at HF/6-31G** and MP2 levels by employing the analytical gradient relaxation method in GAMESS.[17] Three-dimensional visualization of molecules and their respective MESP and PMESP CPs have been effected with UNIVIS[23] visualization program. The 6-31G** basis is chosen since it is known to be adequate[8e] for investigating complexes of simple ions such as Li^+, Na^+, and K^+. Out of these ions, Li^+ is expected to engender a substantial polarization contribution due to its large polarizing ability and has hence been chosen for the present investigation.

Results and Discussion

The salient MESP and PMESP topographical features of the molecules under study are discussed below. The molecules are shown in the figure by ball-and-stick model, and radii of atoms are not according to scale. All MESP and PMESP CPs of isolated hydrocarbons depicted in Figure 1 are exclusively negative-valued ones. Only the CPs of interest are shown in Figure 1 for simplicity. Open and solid circles denote MESP and PMESP CPs, respectively. Stars are used for depicting Li^+ bonded position (within ab initio framework) to the respective hydrocarbons.

The utility of present model can be appraised by comparing parameters obtained by ab initio SCF full optimized parameters of hydrocarbon$\cdots Li^+$ complexes.

(1) CH_4 (Methane). Figure 1a shows that on the C_3 axis of CH_4, the MESP (o) and PMESP (•) minima of values −11.1 and −153.1 kJ mol^{-1} are present, at the distance of 2.01 and 1.22 Å, respectively, from the carbon atom. The PMESP CP is quite deep in value and close to the atom, as noticed earlier by Dehareng et al.[15] for some other molecules, Figure 1b shows the MESP and PMESP saddles present on the C_2 axis of CH_4 located at the distance of 2.05 and 1.25 Å, respectively from C. The corresponding function values are −7.8 and −112.7 kJ mol^{-1}. PMESP CPs present on C_3 axis have more negative function values than respective CPs present on C_2 axis of CH_4. Negative charge is seen to be concentrated on C_3 axis, indicating it to be a more favorable cation binding site.

The model docking interaction energy (ΔE_{dock}) is −38.07 kJ mol^{-1} for Li^+ on C_3 axis, 2.26 Å away from carbon. The value of maximum gradient norm (MGN) turns out to be 0.01 au. In fact, for all the molecules studied here, the MGN lies between 0.01 and 0.02 au, indicating that one indeed has a good starting guess for the complex. Full SCF optimization has been carried out starting with these model docked geometries (cf. Table 1). For the minimum energy structure obtained with full ab initio optimization, the interaction energy (ΔE_{SCF}) is −41.09 kJ mol^{-1}, i.e., ΔE_{dock} is 92.65% of the corresponding ΔE_{SCF} one. The distance of Li^+ from carbon atom in fully optimized structure is 2.24. On the other hand, the interaction energy obtained by docking at MP2 level is −46.92 kJ mol^{-1}, which is 92.8% of full optimized one (−50 kJ mol^{-1}) at the same level. The distance of C$\cdots Li^+$ in this complex, at MP2 level is 2.29 Å.

For inspecting the basis set effect, ab initio calculations have also been carried out at the 6-31++G(d,p) basis set with HF and MP2 level. The interaction energy of full optimized structures are −40.77 and −46.06 kJ mol^{-1}, respectively, quite comparable to the corresponding one at 6-31G** basis set level (viz, −41.09 and −50.56 kJ mol^{-1}). The distance of Li^+ to carbon atom is 2.22 and 2.29 Å at HF and MP2 level, respectively.

A transition state (one imaginary frequency) configuration has been obtained when Li^+ binds along the C_2 axis of CH_4 (cf. Figure 1b), with ΔE_{dock} and ΔE_{SCF} respectively −32.03 and −35.16 kJ mol^{-1}. The distance of Li^+ from carbon in model docked geometry is 2.42 Å, which is very much similar to the one obtained by full optimization (see Table 1). The docking interaction energy at MP2 level is −39.01 kJ mol^{-1}, which is 91.4% of that of a full optimized one. At SCF level, complete optimization binding energy with 6-31++G(d,p) turns out to be −35.22 kJ mol^{-1}, not differing much from respective energy at 6-31G** basis set (cf. Table 1). Considering this experience with the basis set expansion, further work is done only at the 6-31G** basis.

How much role does the basis-set superposition error (BSSE) play in these energetics? The interaction energies of above two configuration of CH_4...Li^+ complex are −43.49 (−46.63) and −37.83 (−40.02) kJ mol^{-1}, respectively, at HF/6-31G** (MP2/

(17) GAMESS − Schmidt, M. W,; Baldridge, K. K.; Boatz, J. A.; Elbert, S. T.; Gordon, M. S.; Jensen, J. H.; Koseki, S.; Matsunaga, N.; Nguyen, K. A.; Su, S. J.; Windus, T. L.; Dupuis, M. Montgomery, J. A. *J. Comput. Chem.* **1993**, *14*, 1347.

(18) The package UNIPROP for mapping MESP and its topography, see Shirsat, R. N.; Bapat, S. V.; Gadre, S. R. *Chem. Phys. Lett.* **1992**, *200*, 373. Program PMESP: for calculation of polarization corrected MESP recently developed in our laboratory in Fortran.

(19) Maron, M. J. *Numerical Analysis: A Practical Approach;* Macmillan: New York, 1982; p 289.

(20) Gadre, S. R.; Bhadane, P. K.*J. Chem. Phys.* **1997**, *107*, 5625.

(21) (a) Kulkarni, S. A. *Chem. Phys. Lett.* **1996**, *254*, 268. (b) Gadre, S. R.; Kulkarni, S. A.; Suresh, C. H.; Shrivastava, I. H. *Chem. Phys. Lett.* **1995**, *239*, 273.

(22) Alkorta, I.; Villar, H. O.; Perez, J. J. *J. Phys. Chem.* **1993**, *97*, 9113.

(23) Limaye, A. C.; Inamdar, P. V.; Dattawadkar, S. M.; Gadre, S. R. *J. Mol. Graph.* **1996**, 14.

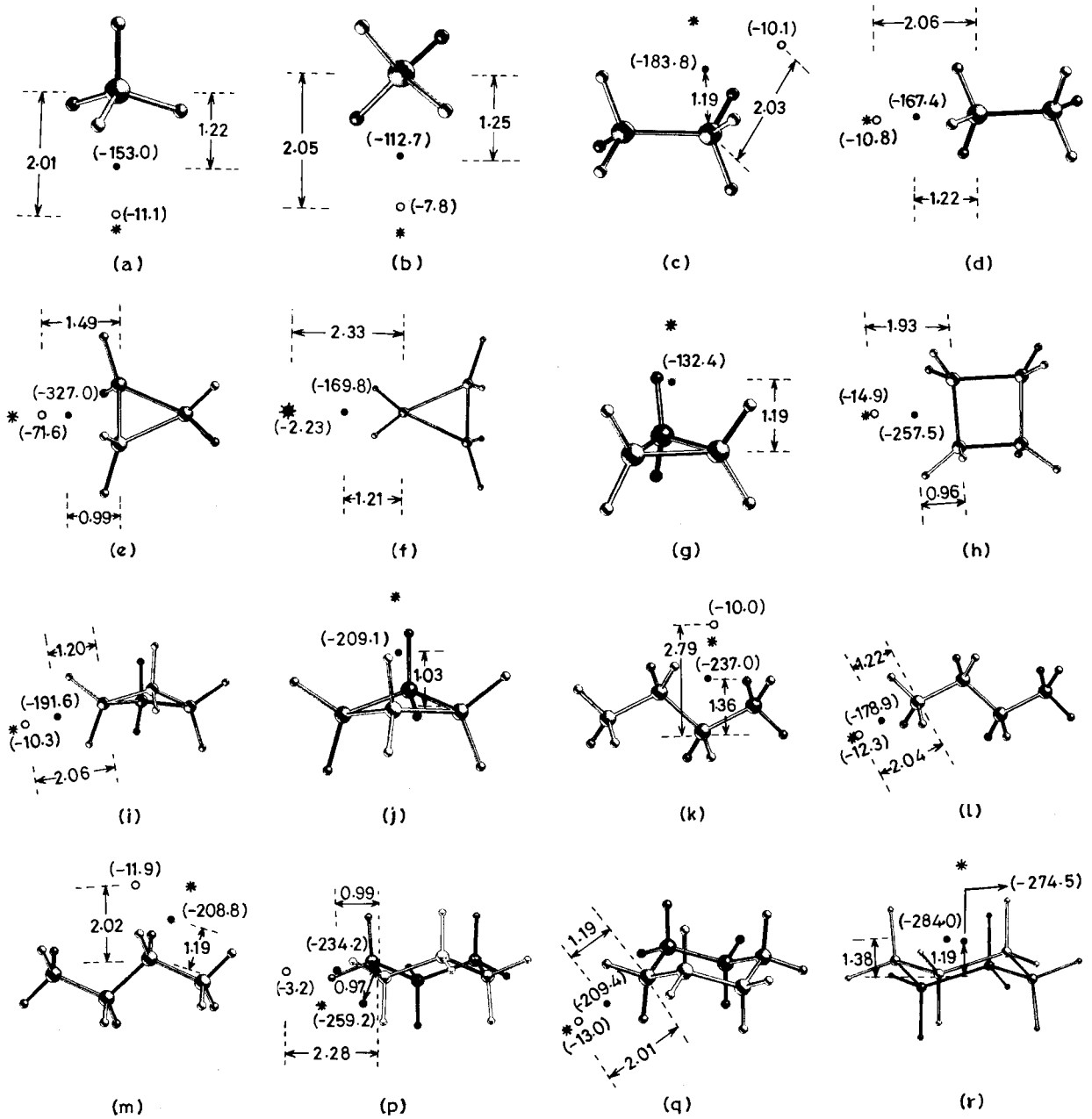

Figure 1. Schematic representation of MESP (○) and PMESP (•) CPs of hydrocarbons and position of Li^+ (*) complexed to the hydrocarbons after full ab initio optimization: methane (a) and (b); ethane (c) and (d); cyclopropane (e), (f), and (g); cyclobutane (h), (i), and (j); *n*-butane (k), (l), and (m); cyclohexane (p), (q), and (r). See text for details.

6-31G**) level with BSSE correction. This shows that BSSE is not very significant and is typically 2.5 (3.5) kJ mol^{-1}. Further, it does not alter the energy rank order of (a) and (b).

(2) C_2H_6 (Staggered Ethane). Figure 1c shows the MESP and PMESP minima with values −10.1 and −183.8 kJ mol^{-1}, respectively. Distances of these CPs from the nearest carbon are 2.03 and 1.19 Å. In Figure 1d it is demonstrated that local minima of MESP and PMESP are present on the C_3 axis of ethane molecule, whose values are −10.8 and −167.4 kJ mol^{-1}. MESP CP present on the C_3 axis in Figure 1d possesses a deeper value than the one which bisects H−C−H angle (Figure 1c). From MESP topographical analysis, it seems that a negative charge is concentrated on the C_3 axis and between two hydrogens of each methyl group. But from PMESP topographical analysis, a more favorable binding site for cation is located perpendicular to the C−C bond, though slightly shifted toward the carbon, where a deeper-valued PMESP CP is located.

After applying the present model, two minimum energy configurations on potential energy surface (PES) are obtained. The complex structure, with Li^+ lying perpendicular to the C−C bond (cf. Figure 1c), has a higher binding energy than the one where Li^+ is bound on the C_3 axis (cf. Figure 1d and Table 1 for geometrical and energetic parameters). It is possible to offer a simple explanation for this on the basis of PMESP topographical analysis. For these configurations, the full optimized binding energies and distances of Li^+ from carbon at MP2 level are −63.37 kJ mol^{-1}, 2.18 Å (Figure 1c) and −60.88 kJ mol^{-1}, 2.21 Å (Figure 1d) respectively, again showing that MP2 level calculations do not affect significantly the geometric parameters as well as trends in binding energies. The binding energy with BSSE correction at HF (MP2) level both with 6-31G** basis for the complex in which Li^+ binds perpendicular to C−C bond of ethane (see Figure 1c) is −55.13 (−59.78) kJ mol^{-1}, whereas the configuration in Figure 1d is −52.25 (−55.58) kJ mol^{-1}.

Table 1. Interaction Energies and Geometrical Parameters in Hydrocarbon···Li^+ Complexes Obtained with 6-31G** Basis Set[g]

location of Li^+	d [R][a]	ΔE_{dock}[b]	ΔE_{SCF}[IMG][c]	ΔE_{MP2}[d]
	CH_4···Li^+			
(a) on C_3 axis	2.26(2.24)[C]	−38.07	−41.09 (0)	−50.58
(b) on C_2 axis	2.42(2.43)[C]	−32.03	−35.16 (1)	−42.67
	C_2H_6···Li^+			
(c) perpendicular to C−C	2.32(2.24)[C−C]	−46.21	−51.23 (0)	−63.37
(d) on the C_3 axis	2.23(2.21)[C]	−47.78	−50.57 (0)	−60.88
	C_3H_6···Li^+			
(e) on C_2 axis perpendicular to C−C	2.10(2.10)[C−C]	−87.69	−94.26 (0)	−108.48
(f) on C_2 axis in region of H−C−H angle	2.35(2.31)[C]	−45.68	−48.84 (1)	−56.75
(g) over the ring	2.31(2.24)[RC]	−33.34	−38.91 (0)	−54.64
	C_4H_8···Li^+			
(h) perpendicular to C−C	2.09(2.07)[C−C]	−68.79	−72.70 (0)	−87.20
(i) in region of H−C−H angle	2.39(2.36)[C]	−51.04	−54.56 (1)	−62.32
(j) over the ring	2.45(2.29)[RC]	−44.82	−55.22 (0)	−66.56
	n-C_4H_{10}···Li^+			
(k) bisecting H−C−H angle of CH_2 and CH_3	2.82(2.75)[C][e]	−68.79	−74.39 (0)	−91.26
(l) at apex of CH_3	2.22(2.20)[C]	−53.82	−56.85 (0)	−67.79
(m) perpendicular to C−C of CH_2 and CH_3, bisecting H−C−H angle of CH_2	2.21(2.21)[C][f]	−57.24	−62.48 (0)	−76.51
	Cyclohexane···Li^+			
(p) perpendicular to C−C	(2.25)[C−C]		−70.81 (0)	
(q) in region of H−C−H angle	(2.35)[C]		−58.26 (1)	
(r) over the ring	(2.26)[RC]		−70.73 (0)	

[a] d, distances of Li^+ from reference point [R] (where R may be a C atom, C−C midpoint or RC ring center) of hydrocarbon in docking model and full optimized ab initio structure, latter in parentheses.) [b] ΔE_{dock}, *single point ab initio* SCF model−docked interaction energy of hydrocarbon···Li^+ complex, at model geometry. See text for details. [c] ΔE_{SCF}, ab initio HF-SCF full optimized bonding energy of hydrocarbon···Li^+ complex and IMG—number of imaginary frequencies. [d] ΔE_{MP2}, ab initio full optimized interaction energy of hydrocarbon···Li^+ complex at MP2 level. [e,f] Carbon of CH_2 group. [g] See text and Figure 1 for details. All distances in Å and energies in kJ mol^{-1}.

This brings out that the trends in interaction energies with and without BSSE are unchanged, and this correction is not very significant for this type of complexes. There is a very small energy difference between the two local energy minima of ethane···Li^+ complex, viz., 0.66 and 2.49 kJ mol^{-1} at SCF and MP2 levels, respectively.

(3) C_3H_6 (Cyclopropane). MESP for this molecule has been discussed by Goldfuss et al.,[13] sans the MESP topography. From our earlier study,[14c] this molecule is known to possess very interesting MESP topographical features. In Figure 1e are shown MESP and PMESP minima present in molecular plane and on the C_2 axis bisecting C−C bond. The function values at these CPs are −71.6 and −327.0 kJ mol^{-1}, and they lie at a distance of 1.49 and 0.99 Å, respectively, from the C−C bond midpoint. Figure 1f has saddle points of MESP and PMESP (connecting these minima) located on the C_2 axis and bisecting the H−C−H angle of cyclopropane. Figure 1g shows that on the top of the ring at the C_3 axis, only a PMESP CP is present (with value of −132.4 kJ mol^{-1}) 1.19 Å away from the center of mass of a cyclopropane molecule. From this analysis, it seems that the cation may prefer to bind strongly perpendicular to the C−C bond on the C_2 axis in the horizontal plane or rather weakly on the same axis but in the region of the H−C−H angle bisector. However, a cation may also bind even more weakly at the top of the ring on C_3 axis.

For the cyclopropane···Li^+ complex, with the present model, these three configurations are probed in which Li^+ shows the strongest interaction energy when it binds in the molecular plane of cyclopropane and perpendicular to the C−C bond (cf. Figure 1e), in which, the docking interaction energy at MP2 level is −102.40 kJ mol^{-1} and after full optimization turns out to be −108.48 kJ mol^{-1}. The structure in which Li^+ occupies a position on the bisector of the H−C−H angle (cf. Figure 1f) has stronger binding than the one where Li^+ sits over the ring (see Figure 1g and Table 1 for energy and geometry parameters). The trends in interaction energies of different configurations of cyclopropane···Li^+ complex are similar to the values of PMESP CPs of cyclopropane (see Figure 1e−g). It may be noted that MESP topographical analysis fails to explain the configuration of the Li^+···cyclopropane complex, in which Li^+ sits over the ring of cyclopropane, due to complete absence of the negative valued MESP region on the C_3 axis of cyclopropane (cf. Figure 1g).

An inspection of the ΔE_{MP2} values shows that the correlation effect is not much significant in this case also.

(4) C_4H_8 (Cyclobutane). Figure 1h depicts negative valued CPs of MESP and PMESP that are present in a direction perpendicular to the C−C bond and in the plane made by midpoints of the four C−C bonds in cyclobutane. Figure 1i displays saddles of MESP and PMESP, which are present in the region of the H−C−H angle. Similar to the case of cyclopropane, negative valued MESP CP on the top of ring is absent, but the PMESP CP is present there (cf. Figure 1j), 1.03 Å away from the center of the mass of cyclobutane of value −209.1 kJ mol^{-1}. With the PMESP topographical analysis, the cation is thus expected to bind most strongly perpendicular to the C−C bond (cf. Figure 1h) followed by the top of the ring (see Figure 1j) and in the region of the H−C−H angle (cf. Figure 1i).

Goldfuss et al.[13] have given MESP maps of planar cyclobutane, in which negative valued regions are not mentioned. Hence it is not clear why Li^+ binds to cyclobutane. With the present method, three configurations of cyclobutane···Li^+ complex have been probed (see Figures 1h−j).

The energy difference between two SCF-level minima on PES of structure in Figure 1(parts h and j) for cyclobutane···Li^+ complex is 17.48 kJ mol^{-1}, only one-third that for the C_3H_6··· Li^+ complex.

(5) n-C_4H_{10} (n-Butane). Figure 1k brings out a saddle point of MESP and a minimum of PMESP bisecting the H−C−H angle of CH_3 and middle CH_2 groups and in the least-squares

plane (LSP) passing through the carbon framework. Values of terminal CH_3 group minima of MESP and PMESP depicted in Figure 1l are −12.3 and −178.9 kJ mol^{-1}, which are in the LSP passing through the carbon framework. Figure 1m represents a minimum of MESP which is present in the region of the H−C−H angle CH_2 group and in the LSP passing through the carbon framework of value −11.9 kJ mol^{-1}. In a similar plane, minimum of PMESP is present along a line almost perpendicular to C−C bond, although slightly shifted toward the CH_2 group (cf. Figure 1m). Specifically from MESP topographical analysis, a cation may bind strongly to the apex of CH_3 group followed by the region of the H−C−H angle of the CH_2 group and in the vicinity of the MESP saddle depicted in Figure 1m. On the other hand, the PMESP topographical analysis predicts the cation to bind near the lowest minimum (Figure 1k) followed by a local minimum (Figure 1m) and then in the region of the terminal methyl group (cf. Figure 1l).

Three minimum energy configuration on PES are obtained (see Figure 1k−m). The present model is seen to work well for giving an initial guess for full optimization of these configurations (cf. Table 1). The values of PMESP CPs of *n*-butane show trends parallel to the interaction energies of the respective complex structures (see Table 1 and Figure 1k−m), whereas MESP topographical analysis fails to explain that.

Energy differences between these configurations on PES are −17.54, −11.91 and 5.63 kJ mol^{-1} between pairs of configuration in Figure 1(parts k and l, k and m, and l and m, respectively).

(6) C_6H_{12} (Cyclohexane). Figure 1p−r depicts the MESP and PMESP CPs of this cyclic saturated hydrocarbons. The MESP fails to show detailed topographical features: it shows a saddle on a line perpendicular to each C−C bond and a minimum each around the H−C−H angle bisector (cf. Figure 1 (parts p and q)). On the other hand, PMESP exhibits five distinct CPs, which are not related by symmetry. The most negative CP happens to be over the ring with a value of −284.0 kJ mol^{-1} accompanied by a closely spaced saddle point on the S_6 axis with a value of −274.5 kJ mol^{-1}. Two PMESP saddles are observed approximately bisecting the H−C−H angle and perpendicular to the C−C bond, respectively (with values of −209.4 and −234.2 kJ mol^{-1}, respectively). A minimum corresponding to the PMESP value of −259.2 kJ mol^{-1} is observed perpendicular to C−C bond, shifted toward carbon, outside the C−C bond, and above the plane made by midpoints of C−C bonds. In the region, guided by three PMESP CPs, three structures of cyclohexane···Li^+ are obtained (cf. Table 1). Two of these structures are extremely close in energy (differing only by about 0.1 kJ mol^{-1}). In the other structure, Li^+ binds in the region of the H−C−H angle with lesser interaction energy compared to the above two structures. Purely MESP based description would have predicted maximum binding energy for Li^+ in this region.

Is there any simple way of predicting the complexation energies from the corresponding PMESP minimum value? Figure 2 shows a plot of PMESP CP values of hydrocarbons vs the corresponding fully ab initio optimized interaction energies of hydrocarbon···Li^+ complexes at HF/6-31G** level. The correlation coefficient and slope of this line turn out to be 0.97 and 0.27, respectively. A similar correlation coefficient is obtained even when the MP2 interaction energies are plotted vs the PMESP values, but the slope of the line in this case is 0.31. The corresponding plot of interaction energies at HF level vs MESP shows rather erratic behavior with a correlation coefficient of approximately 0.70. In addition, many a time, the MESP CPs are conspicuous by their absence for the corresponding hydrocarbon···Li^+ optimized structures. This strongly supports our view that PMESPs of hydrocarbons offer a reliable tool for evaluation of the binding energies with cations.

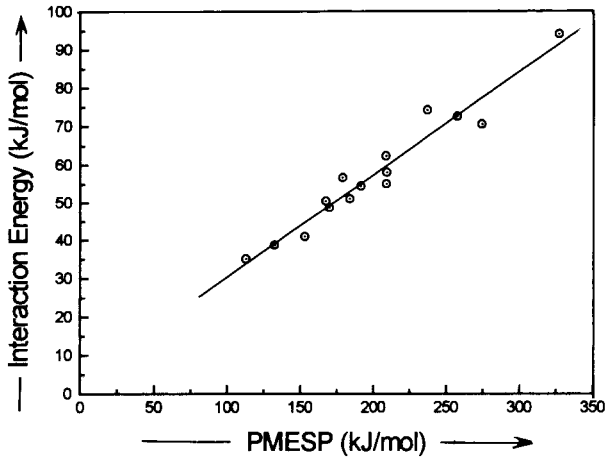

Figure 2. Linear correlation between ab initio (HF/6-31G**) binding energies of Li^+ with hydrocarbon complexes and the corresponding PMESP values at CPs. See text for details.

Table 2. Kitaura−Morokuma (KM) Energy Decomposition Analysis of Some of the Hydrocarbon···Li^+ Complexes, at HF/6-31G** Level[b]

complex[a] structure	ES	EX	PL	CT	MIX	ΔE_{KM}
CH_4···Li^+ (a)	−18.31	17.67	−40.98	−19.84	17.10	−44.36
C_2H_6···Li^+ (c)	−15.88	22.21	−58.15	−26.43	22.05	−56.20
C_3H_6···Li^+ (e)	−65.54	35.30	−67.53	−28.83	25.47	−101.16
C_3H_6···Li^+ (f)	−10.07	17.83	−56.86	−24.29	21.49	−51.90
C_3H_6···Li^+ (g)	8.18	18.89	−64.50	−32.93	26.05	−44.32
C_4H_8···Li^+ (h)	−25.29	27.87	−81.74	−32.18	34.81	−76.52
C_4H_8···Li^+ (j)	−1.90	23.16	−80.86	−36.93	32.59	−63.94

[a] Cf. Figure 1 and Table 1 for a detailed description of geometries of the complexes. [b] All energies in kJ mol^{-1}.

Our approach of mapping of PMESP in three dimensions is thus seen to yield a meaningful picture of potent cation coordination sites. It is possible to predict, semiquantitatively, probable cation binding sites in saturated hydrocarbons, on the basis of their PMESP study and employing ab initio SCF molecular docking by moving the Li^+ ion on a line as explained in the earlier section.

Mecozzi et al.[5b] have recently noticed a very good correlation between the interaction energy for complexes of Na^+ with aromatic systems and the corresponding MESP value at a point conveniently chosen over the aromatic ring. Naphthalene shows deviation from correlation line, on which they have noted that other than electrostatics, polarizability-related terms are important. They have further noted that polarization will also contribute to binding energies for C_6H_6···NMe_4^+ complexes.

The hydrocarbon···Li^+ systems were subjected to a detailed Kitaura−Morokuma[24] (KM) decomposition analysis in order to assess significance of the relative weightages of various factors, such as electrostatics (ES), exchange (EX), polarization (PL), and charge transfer (CT) in the interaction energy (E_{KM}). This analysis was carried out using GAMESS[17] package, and the results are summarized in Table 2. It may be noticed from Table 2 that PL is indeed a dominant term followed by CT, EX, and MIX (which signify other contributions than ES, EX, PL, and CT) terms. Electrostatic term shows wide oscillations; it is indeed dominant for C_3H_6···Li^+ global minimum structure but

(24) Kitaura, K.; Morokuma, K. *Int. J. Quantum Chem.* **1976**, *10*, 325.

is even positive for the on top structure for this species. This indeed brings out the features revealed by MESP maps, viz., the strong π character of cyclopropane in plane of ring, but no negative potential over the ring. It may be noted that the interaction energies in Tables 1 and 2 differ from each other since the KM analysis employs energies of monomers as they exist in dimers.

In recent years,[25] it has been realized that there are several limitations of KM analysis, e.g., the analysis is done from the wave function which is not antisymmetric, i.e., it does not satisfy the Pauli exclusion principle. Thus the results in Table 2 are only indicative and need not be taken as a result of a unique and rigorous decomposition scheme. There are some better methods available for the decomposition analysis. However, the results of KM analysis indicate that polarization and, selectively for some structures, electrostatics are quite significant terms. The exchange and charge-transfer terms taken together show a lot of cancellation.

Concluding Remarks

The important role of electrostatics in weak intermolecular complexation[14c] as well as in cation-π complex formation[5b,6b,8b,c] has been emphasized in the earlier literature. In fact, the complementary electrostatic features in the weak intermolecular complexation processes have been exploited by the Buckingham and Fowler (B−F)[26] as well as EPIC[14c,27] models. For the case of saturated hydrocarbons, however, the polarization seems to play an important role. In view of this, the critical points of PMESP for methane, ethane, cyclopropane, cyclobutane, *n*-butane, and cyclohexane are employed for prediction of probable sites of coordination of a small cation, viz., Li^+. The Kitaura−Morokuma analysis of the results indeed brings out this fact. However, the electrostatic term does dominate in the systems which are classically endowed with a π like character, e.g., cyclopropane. The interaction energies predicted by simple docking procedure outlined here turn out to be 90% of the final optimized ones. The enhancement of the basis as well as inclusion of correlation does not seem to qualitatively affect the binding energy values. The conclusion that the polarization as well as electrostatic terms plays an important role in the species is in agreement with the references noted earlier.[1a,2d,g,4,6b,7b,9] Our conclusions are also in general agreement with the observation of Hill et al.[2g] that the binding energy of Li^+ increases with the size of the hydrocarbon size. For systems such as benzene and substituted benzene, however, the electrostatic effect would dominate over those in cyclohexane, as noted recently by Mecozzi et al.[8c] We have already seen this occur in the case of cyclopropane which is classically known to possess a significant π character.

A noteworthy outcome of the present work is the linear plot of interaction energies of hydrocarbon···Li^+ complexes and the corresponding PMESP CP values of the respective hydrocarbon. This indeed could be exploited for a prediction of binding energies without actually doing full SCF/MP2 geometry optimizations. How useful is the present approach for more diverse chemical systems? Our preliminary investigations[28] on Li^+ binding to ethylene and HCN indicate no significant deviation from the straight line in Figure 2. Further studies with a wide variety of molecules are in progress.

In summary, the polarization-corrected molecular electrostatic potential seems to offer better primitive patterns of understanding for the cation binding problem, especially where a pure molecular electrostatics-based approach seems to fail.

Acknowledgment. Support from the Council of Scientific Research New Delhi [1(1430)/96-EMR-II) and 9/137(286)/96-EMR-I] is gratefully acknowledged.

JA971544C

(25) Chen, W.; Gordon, M. S. *J. Phys. Chem.* **1996**, *100*, 14316.

(26) (a) Buckingham, A. D.; Fowler, P. W. *Can. J. Chem.* **1985**, *63*, 2018. (b) Buckingham, A. D.; Fowler, P. W. *J. Chem. Phys.* **1983**, *79*, 6426.

(27) Gadre, S. R.; Pundlik, S. S. *J. Phys. Chem.* **1997**, *101*, 3298.

(28) Gadre S. R.; Pingale S. S. (unpublished).